MULTIPHASE SLUG FLOW-ENHANCED INTERNAL CORROSION OF CARBON STEEL PIPELINES IN SWEET PRODUCTION SYSTEMS

MADAN GOPAL
NSF I/UCRC, CORROSION IN MULTIPHASE SYSTEMS CENTRE
INSTITUTE FOR CORROSION AND MULTIPHASE TECHNOLOGY OHIO UNIVERSITY, ATHENS-45701, USA

ABSTRACT

This paper presents the results of extensive research in multiphase flow-enhanced corrosion in 10-cm diameter, high pressure pipes at elevated temperature under conditions representative of flow lines in the field. Mixture of oil and ASTM substitute seawater has been used in the liquid phase and carbon dioxide has been used in the gas phase. Detailed experimental data have been collected on the multiphase flow characteristics, including, flow regimes and their transitions, velocities and holdups, and their effect on the turbulence resulting in the highly enhanced corrosion in these lines. Pressure drop and mass transfer measurements have been made to quantify these effects. Corrosion rates have been measured to determine the effect of multiphase flow on corrosion and predictive models have been developed for the oil and gas industry.

The most severe flow regime from a corrosion point of view is slug flow. Results show that slug flow involves the entrainment of large amounts of gas into the liquid. This is released into a turbulent mixing zone in the form of pulses of bubbles. These bubbles do impact and collapse on the bottom of the pipe, causing a cavitation-type localized corrosion/erosion damage. This removes corrosion product and inhibitor films from the surface that could otherwise have protected the pipe from further corrosion. Instantaneous peaks in wall shear stress and current density of the order of 100-1000 times the average have been seen. These are consistent with bubble collapse mechanisms. The results in slug flow have been modeled using a dimensionless Froude number and it has been shown that the slug characteristics and corrosion rates are strong functions of the Froude number. Results are presented for carbon dioxide partial pressures up to 0.79 MPa and temperature up to 100 °C.

INTRODUCTION

Multiphase flow is now a common occurrence in offshore oil and gas production. Full well stream system and long-distance multiphase flowlines are already in operation in many parts of the world and now being routinely considered during design of future systems. Internal corrosion problems in these lines and the technical challenges involved in their corrosion inhibition are also well known. Proper understanding of the underlying mechanisms governing corrosion in multiphase flow is crucial to the implementation of effective inhibition programs necessary for safe and profitable operation of existing lines and the development of new fields.

As the well gets depleted, enhanced oil recovery methods, involving the injection of carbon dioxide and seawater into the reservoir, are used. This helps maintain the pressure within the reservoir. However, the carbon dioxide and brine then flow with the oil and gas and the resulting multiphase mixture can cause severe internal corrosion of the pipelines. Many wells operate at water cuts as high as 98 %. The carbon dioxide dissolves in the seawater and forms weak carbonic acid. This acid is corrosive and leads to higher corrosion rates in carbon steel pipelines. Many researchers have investigated the mechanism of carbon dioxide corrosion. Some of the workers include de Waard and Milliams (1975), Ikeda et al. (1985), Ogundele and White (1986), Videm and Dugstad (1989), de Waard, Lotz and Milliams (1991), de Waard and Lotz (1993), and de Waard, Lotz, and Dugstad (1995). Currently, most oil and gas companies use their own modified versions of the carbon dioxide corrosion models developed by the de Waard group.

The strategy to combat corrosion problems is to use carbon steel pipes but reduce and, if possible, prevent the rate of material losses through the use of corrosion inhibitors. The inhibitors act by bonding to the metal surface and forming a protective film. The performance of the inhibitor depends on the metal surface, inhibitor composition, and fluid flow conditions. Some of the inhibitors are not effective because of the multiphase flow conditions in the pipelines. While selecting an inhibitor, it is essential to know its effectiveness in the specific service environment. A detailed knowledge of the metal surface conditions, operating temperature and pressure, fluid properties, the solution pH, and the multiphase flow conditions are essential.

Multiphase Flow

Multiphase flow involves the simultaneous flow of more than one phase within a pipe. This includes two-phase oil/gas and oil/water flows and three-phase oil/water/gas flows.

Several flow patterns exist in multiphase flows. It must be noted that the flow is seldom homogeneous and, in most cases, different velocity and phase fractions exist at any given location within the pipe. This is fundamentally different from single-phase flow. Also, in most cases, the flow is turbulent.

Three Phase Oil/Water/Gas Flows

Figure 1 shows a schematic of three-phase oil/water/gas flow patterns (Lee and Jepson, 1993). At low gas and liquid velocities, a stratified layer of liquid flows under the gas, the interface between the two layers is smooth. An increase in the gas velocity leads to the formation of regular two-dimensional waves at the gas-liquid interface. These regime is smooth and wavy-stratified flow. With further increase in gas velocity, the two-dimensional waves grow in height and begin to roll over, acquiring a three-dimensional character. This is called the rolling wave. At higher liquid velocity, there is a transition from stratified to an intermittent flow pattern. The waves on the liquid layer grow to bridge the pipe and block the gas. This results in the flow of intermittent pockets of gas separated by lumps of liquid. At low gas velocities, plug flow occurs. The plug flows over the liquid film intermittently between elongated gas bubbles, with very little turbulence.

At higher gas velocities, the front of the plug begins to overrun the liquid film and assimilates it in the process. This regime is called slug flow and is the most important flow regime from a corrosion viewpoint. With further increase in gas velocity, large three-dimensional roll waves appear on the liquid film between slugs. The slugs are highly aerated and this regime is called pseudo-slug flow. On further increase in the gas velocity, blow-through occurs, with the gas flows in the central core of the pipe, with a thin layer of liquid flowing in the annulus around it. This regime is called annular flow. A flow regime map depicts the type of flow pattern present in a pipeline at a particular liquid and gas velocity.

It is to be noted that a separate water layer is always present at the bottom of the pipe in all the flow regimes. This layer exists even at water cuts as low as 10% and measurable corrosion can occur in multiphase flow.

Flow Regime Map

Figure 2 shows a flow regime transition map for three-phase oil/water/gas flow in a 30-cm (12-inch) diameter pipe at a pressure of 0.79 MPa (100 psig) with 50% water in the liquid phase (Laws, 1999). The oil viscosity is 2 cp. Carbon dioxide is used in the gas phase. It is seen that slug flow occurs at liquid velocities greater than 0.2 m/s and no slug/annular flow transition is seen. Also, most pipelines will experience some slight changes in inclination. Inclination has a dramatic effect on multiphase flow regimes. Figure 3 shows a flow regime transition map for a 2° upward inclined pipe (Maley, 1997). It is seen that within the range of velocities normally seen in industrial pipes, the most dominant flow regime is slug flow. In fact, an inclination of even $+0.5^\circ$ eliminates stratified flow and slug flow predominates. This is important from a corrosion point of view, since slug flow results in dramatic increases in corrosion rates.

Slug Flow

Slug flow exists in pipelines carrying oil and gas when high production of oil and gas is required. Slug flow is characterized by the appearance of intermittent liquid slugs that propagate through the pipe. An idealized slug unit is shown in Figure 4 and consists of four zones (Jepson, 1986). Ahead of the slug is a slow moving liquid film, with gas flowing above it. Waves are formed on this film and grow to bridge the pipe. They are then accelerated to the gas velocity and form the slug. The front of the slug overruns the slow moving film ahead of it and assimilates it into a mixing zone behind the front, creating a highly turbulent region. This highly turbulent mixing zone entrains gas, which is passed back into the slug body. Here the turbulence is reduced, and eventually the liquid velocity is reduced to a point where it is no longer able to sustain the bridging of the pipe. This is the tail of the slug. Liquid is shed from the tail of the slug to a trailing film. This liquid in turn mixes with more incoming liquid to form a film on which the next slug will propagate. The intensity of turbulence within the slug can be determined using a dimensionless Froude number (Kouba and Jepson, 1987) in the stratified liquid film ahead of the slug:

$$Fr_f = \frac{v_t - v_{LF}}{\sqrt{g\, h_{EF}}} \tag{1}$$

where,

Fr_f	=	Froude number in the liquid film ahead of the slug
v_t	=	translational velocity of the slug
v_{LF}	=	velocity of the liquid film ahead of the slug
h_{EF}	=	effective height of the liquid film ahead of the slug (Calculated as area of liquid film divided by the width of the gas-liquid interface)

Effect of Slug Flow on Corrosion

Extensive research has been carried out at the Institute on slug flow characteristics and their effects on corrosion rate. Zhou and Jepson (1994) demonstrated that corrosion rate increases with Froude number due to increase in void fraction entrained within the slug and associated increased turbulent intensity and wall shear. Gopal et al. (1995) described the mechanisms governing the enhanced corrosion in multiphase slug flow using video images of moving slugs. . As the front rolls over and assimilates the slow moving liquid film ahead, it accelerates and entrains large amounts of gas in the process. The gas is then released into the slug in the form of pulses of bubbles within a highly turbulent mixing vortex that is created just behind the slug front as shown in Figure 5. The pulse is caught in the wake of the mixing vortex and is forced towards the bottom of the pipe. The bubbles impact on the pipe wall and collapse, causing a cavitation-type effect, which is the primary mechanism causing the severely enhanced corrosion in multiphase slug flow. Details of the mixing zone are given by Gopal (1997, 1998 a and b). Bhongale (1996) investigated the effect of slug flow on corrosion at different pressures, temperatures and water cuts. He developed a predictive model for corrosion rate in multiphase slug flow. The model has been extended to include the effects of slug frequency (Jepson et al., 1997) and liquid viscosity and gas density (Jepson et al., 1998). The effect of multiphase slug flow on corrosion in inclined pipes was also studied by Gopal et al. (1998). They found that slug frequency and Froude number were higher in inclined pipes at the same flow rates when compared with horizontal pipes, resulting in higher corrosion rates. Gopal and Rajappa (1999) studied carbon dioxide corrosion of steel pipes in slug flow under scale forming conditions. They found that the corrosion rate reduced to negligible values under full pipe flow but substantial corrosion was still observed in slug flow. Clear evidence of damage to corrosion product layers was observed.

EXPERIMENTAL SETUP

The experiments will be performed in an 18-m long, 10-cm diameter, high pressure, high temperature, inclinable flow loop shown in Figure 6. The entire system is manufactured from 316 stainless steel. A brine/oil solution is stored within a 1.4 m^3 mixing tank. The liquid is moved through the system by a 3 - 15 kW variable speed centrifugal pump. The flow is then controlled within a range of zero to 100 m^3/hr with the variable speed pump in conjunction with a recycle stream. The recycle stream and return stream also serve to agitate the liquid in the mixing tank. Flow rate is metered with a GH-Flow Automation TMTR510 Frequency Analyzer coupled with an in-line turbine meter. A feed line at 2 MPa pressure supplies carbon dioxide gas from a 20,000 kg storage tank. After passing through a pressure regulator, the gas flow rate is metered with an HEDLAND variable area flow meter where the pressure and temperature are also measured. The gas then passes through a check valve and is mixed with the liquid. The multiphase flow then enters the test loop. The pipe inclination can be set at any angle from 0° to 90°. Both upward and downward flows are studied simultaneously.

The test section is shown in Figure 7. Electrical resistance (ER) probes are inserted flush with the pipe wall to determine corrosion rates. The flow regime and Froude number is determined using a patented (US Patent 5,708,211, 1998) nonvisual technique, combined with a patented ultrasonic technique (US Patent 5,719,329, 1998). In addition, the system pressure, pH and temperature are also noted.

Test Matrix

The experimental fluids and conditions are listed in Table 1.

Table 3.1 TEST MATRIX

PARAMETER	CONDITIONS
Temperature, C	40, 60 and 80
CO_2 partial pressure, MPa	0.27, 0.45 and 0.79 MPa
Water cut	40 and 80 %
Froude number	6, 9 and 12
Aqueous phase	ASTM substitute seawater
Oils	Simulated light crude (μ: 2 cP at 40 C) Simulated moderately viscous crude (μ: 100 cP)

RESULTS

Figure 8 shows the effect of Froude number on the void fraction at the bottom of the pipe at different conditions of temperature and carbon dioxide partial pressure for 40% water cut. It is seen that the amount of gas entrained increases with Froude number. This is due to the increased turbulence. As the temperature increases, the viscosity of the liquid mixture decreases resulting in even higher levels of turbulence. For example, at a temperature of 80 C and pressure of 0.79 MPa, the void fraction at the bottom increases from 0.05 to 0.07 and then to 0.11 as the Froude number is increased from 6 to 9 and then to 12. The variation of pressure drop and turbulence across the slug is clearly seen from Figure 9. At 40% water cut and a temperature of 40 C, at a pressure of 0.45 MPa, the pressure drop increases from 2.32 to 3.65 kPa as the Froude number is raised from 6 to 12. It is also seen from Figure 9, that the pressure drop increases with pressure at the same Froude number. For example, at Froude number 9, the pressure drop increases from 2.31 kPa to 2.70 kPa and then to 3.46 kPa, as the pressure is increased from 0.27 to 0.45 and then to 0.79 MPa. This is due to increased gas density, which increases the turbulence and shear associated with gas entrainment at the higher pressures.

The effects of the slug characteristics on corrosion rate can be seen from Figure 10, which shows the variation of corrosion rate as a function of temperature at different pressures and Froude numbers. The corrosion rate increases with temperature due to two reasons. There is a kinetic effect of temperature and the increased turbulence effect discussed above. Comparison with full pipe oil/water flows at the same temperature and pressure shows that there is a significant effect of slug flow (Kanwar, 1994). No maximum is observed in the corrosion rate. Figure 11 shows a comparison of corrosion rates using different oils and gases. It is seen from Figure 11, that at a water cut of 40%, at a temperature of 80 C and pressure of 0.79 MPa (100% carbon dioxide), for a Froude number of 12, the corrosion rate with a 2 cp oil was 33.5 mm/yr. Under the same conditions, but the carbon dioxide partial pressure kept constant at 0.27 MPa (with total pressure at 0.79 MPa) the corrosion rate is 11.7 mm/yr. This shows that there is significant effect of slug flow turbulence on the corrosion even at low carbon dioxide partial pressures. The corrosion rates with a 2 cP oil increase rapidly with temperature, due to the significantly higher turbulence.

Rajappa (1999) has performed corrosion experiments in slug flow under scaling conditions. He found that under full pipe oil/water flows, the corrosion rate decreases to negligible values with increasing iron content in the system. However, significant corrosion still existed in slug flow. This is seen from Figure 12, which shows the variation of corrosion rate with temperature. The corrosion rate is found to be 12.1 mm/year at 60 C while it increases to 14.2 mm/year at 80 C. The same trend is observed at Froude numbers 6 and 12. At 60 C and Froude number 6, other conditions remaining constant, the corrosion rate is 11.2 mm/year and increases to 13.0 mm/year at 80 C. Also, at 60 C and Froude number 12, the corrosion rate is 13.2 mm/year and increases to 15.4 mm/year at 80 C. Pitting occurs on the surface of the film as a result of bubble impact on the pipe bottom. These bubbles impact on the bottom and could possibly collapse, resulting in a large force sufficient to cause pitting on the corrosion film. Figure 13 shows bubble impact on the corrosion film and a pit formation under slug flow conditions at 0.27 MPa, 80 °C, 80 % water cut at Froude numbers 12. Currently, research is underway at the Center in collaboration with the University of Central Florida to characterize the microstructural damage and porosity of these films and the impact of the multiphase slug flow on the inhibitor films that may form on these surfaces. Figure 14 shows instantaneous mass transport values in slug flow at a Froude number of 9 (Jiang and Gopal, 1998). It can be seen that peaks 10-100 the average value are observed at regular intervals. These correspond to the pulses of bubbles within the mixing zone of the slug. The bubbles impact on the surface resulting in such enormous increases in mass transfer and the associated corrosion rates.

CONCLUSIONS

Results of multiphase flow-enhanced sweet corrosion in high pressure, three phase oil/water/gas slug flow at elevated temperatures are presented. Multiphase flow regimes are described and the effects of pipe geometry and inclination on the regimes are shown.

The most severe flow regime from a corrosion point of view is slug flow. This regime involves entrainment of large amounts of gas within the liquid, which are released into a turbulent mixing zone in the form of pulses of bubbles. Their effect on the turbulence results in the highly enhanced corrosion in these lines. Pressure drop and mass transfer measurements have been made to quantify these effects. Corrosion rates have been measured to determine the effect of multiphase flow on corrosion and the effect of the slug characteristics on corrosion have been described.

Results show that gas bubbles do impact and collapse on the bottom of the pipe, causing a cavitation-type localized corrosion/erosion damage. This removes corrosion product films from the surface that could otherwise have protected the pipe from further corrosion. Instantaneous peaks in wall shear stress and current density of the order of 100-1000 times the average have been seen. These are consistent with bubble collapse mechanisms. The results in slug flow have been modeled using a dimensionless Froude number and it has been shown that the slug characteristics and corrosion rates are strong functions of the Froude number.

REFERENCES

1. Bhongale, S., "Effect of Pressure, Temperature and Froude Number on Corrosion Rates in Horizontal Multiphase Slug Flow", M. S. Thesis, Ohio University, 1995.
2. De Waard, C., and Milliams, D.E., "Carbonic acid corrosion of steel. Corrosion", Vol. 31, no. 5, pp. 177-181, 1975.
3. De Waard, C., Lotz, Milliams, D. E.,, Prediction model for CO_2 corrosion engineering in wet gas pipelines, Corrosion, Vol. 47, no. 12, pp 976, 1991.
4. De Waard, C., Lotz, U., "Prediction model for CO_2 corrosion of carbon steel", Corrosion '93, paper no. 69, 1993
5. De Waard, C., Lotz, U., and Dugstad, A., "Influence of liquid flow velocity on CO_2 corrosion: a semi-empirical model", Corrosion, 128/1 - 128/15, 1995.
6. Gopal and co-workers, "Ultrasonic Measuring System & Method of Operation", US Patent no. 5,719,329, 1998.
7. Gopal, M., and Jepson, W. P., "Development of Digital Image Analysis Techniques for the Study of Velocity and Void Profiles in Slug Flow", Int. J. Multiphase Flow, Vol. 23, No. 5, pp. 945-965, 1997.
8. Gopal, M., and Jepson, W. P., "Study of Dynamic Slug Flow Characteristics using Digital Image Analysis, Part I: Flow Visualization and Part II: Modeling Results", *Journal of Energy Resource and Technology*, Vol. 120, pp. 95-107, June 1998.
9. Gopal, M., and Rajappa, S., "Effect of Multiphase Slug Flow on the Stability of Corrosion Product Layer", Corrosion/99, paper no. 46, 1999.
10. Gopal, M., Kang, C., Maley, J., Jepson, W.P., "Sweet Corrosion in Large Diameter, Inclined Multiphase Pipelines," NACE Eighth Middle East Corrosion Conference, Bahrain, May 1998.
11. Ikeda, A, Ueda, M and Mukai, S, "CO_2 behavior of carbon and Cr steels", Advances in CO_2 corrosion, Vol. 1, NACE, Houston, TX, 1985.
12. Jepson and co-workers, "Flow Regime Determination & Flow Measurement in High Pressure Multiphase Pipelines", US Patent no. 5,708,211, 1998.
13. Jepson, W. P., "The Flow Characteristics in Horizontal Slug Flow", 3rd International Conference on Multiphase Flow, Hague, Netherlands, Paper F2, 1987.
14. Jepson, W. P., Krishnamoorthy, V., Gopal, M., "Modelling of Multiphase Slug Flow Characteristics and Their Influence on Corrosion in Large Diameter, High Pressure Horizontal Pipelines," NACE Eighth Middle East Corrosion Conference, Bahrain, May 1998.

15. Jepson, W. P., Lee, A-H., Sun, J-Y., "Study of Flow Regime Transitions of Oil-Water-Gas Mixtures in Horizontal Pipelines," *Proceedings of the International Society of Offshore and Polar Engineers*, (ISOPE), Paper No. JSC-052, Singapore, June 1993.
16. Jepson, W. P., Stitzel, S., Kang, C., Gopal, M., "Model for Sweet Corrosion in Horizontal Multiphase Slug Flow", Corrosion/97, paper no. 11, 1997.
17. Jiang, L., and Gopal, M., "Calculation of Mass Transfer in Multiphase Flows," Corrosion/98, paper no. 50, 1998.
18. Kanwar, S., "Study and Modeling of Sweet Corrosion of Multiphase Mixtures in a Horizontal Pipeline", M. S. Thesis, Ohio University, 1994.
19. Kouba, G.E., Jepson, W.P., "Slugs and Hydraulic Jumps in Horizontal Two Phase Pipelines," 4th International Conference on Multiphase Flow, Paper H1, Nice, France, June 1989.
20. Laws, J., "Localized, Flow Dependent, Sweet Corrosion at Regions of Drastic Changes in Elevations: Hilly Terrain, and River Crossings", M.S. Thesis, Ohio University, 1999.
21. Ogundele, G. I., and White, W.E., "Some observations on corrosion of carbon dioxide in adequate environments containing carbon dioxide", Corrosion, 42, (2), pp. 71-78, 1986.
22. Rajappa, S., "Stability of Corrosion Layers at High Pressure and Temperature Multiphase Flow Conditions", M. S. Thesis, Ohio University, 1999.
23. Videm, K and Dugstad, A, "Corrosion of carbon steel in an aqueous carbon dioxide environment. Part 1: Solution effects", Material Performance, 63 – 67, 1989.
24. Zhou X-L, and Jepson, W.P., "Experimental Study of Multiphase Slug Flow Characteristics and their Effect on Corrosion in Pipelines," NACE International Annual Conference and Exhibition, Paper No. 92081, Nashville, TN, April 1992.

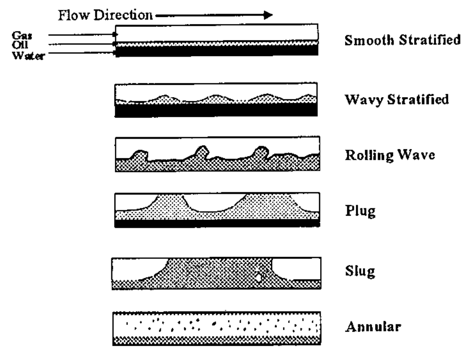

Figure 1: Schematic of horizontal three phase (gas-oil-water) flow pattern

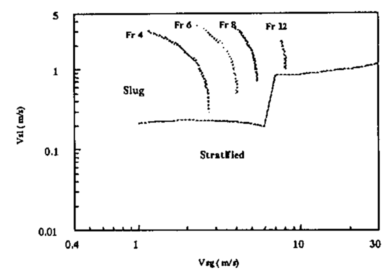

Figure 2: Froude number isoclines in a 12 inch horizontal pipe at 100 psig
The oil viscosity is 2 cP and the water cut is 50%

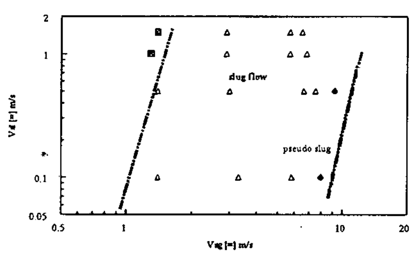

Figure 3: Flow regime map for 40% ASTM seawater, 2° inclination, 0.27 MPa

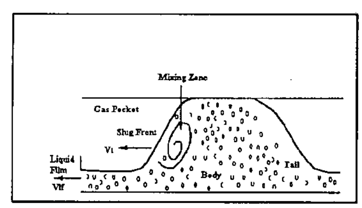

Figure 4: Profile of the different regions within the slug

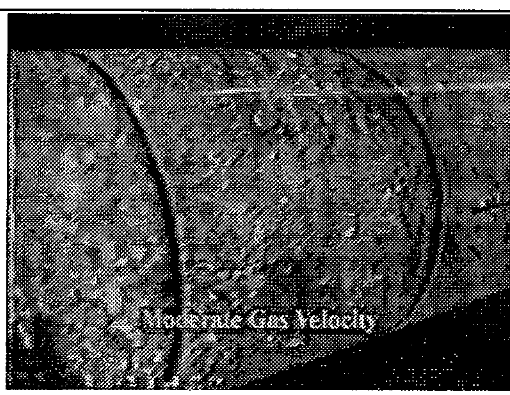

Figure 5: Mixing zone of slug

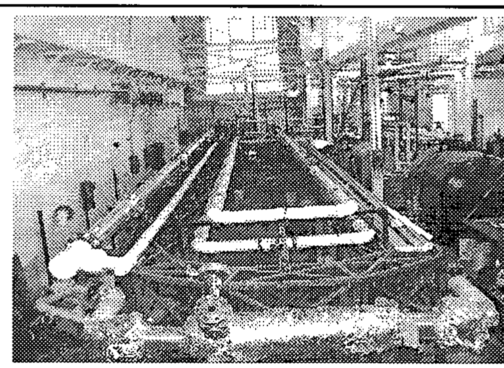

Figure 6: Experimental Multiphase Flow System

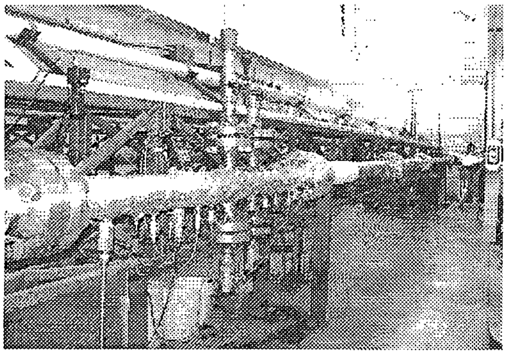

Figure 7: Test section

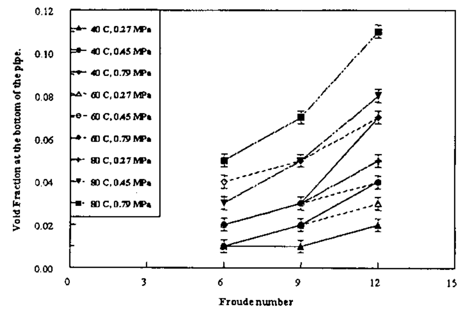

Figure 8: Effect of Froude number on void fraction at the bottom of the pipe at different pressures and temperatures at 40% water cut

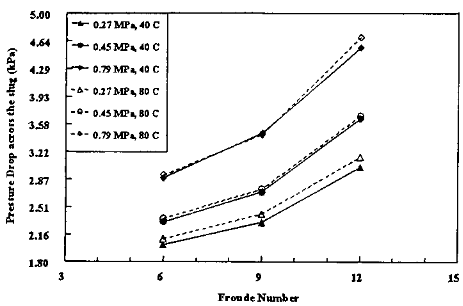

Figure 9: Variation of pressure drop across the slug with Froude number (at 40 C and 80 C) at 40% Water Cut

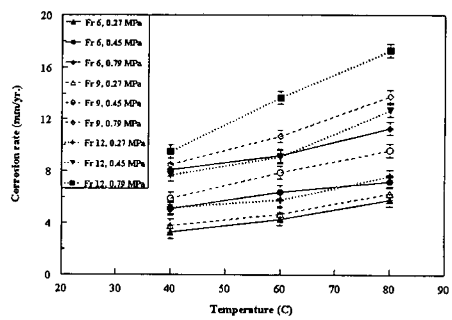

Figure 10: Effect of temperature on corrosion rate at different pressures and Froude numbers at 40% water cut

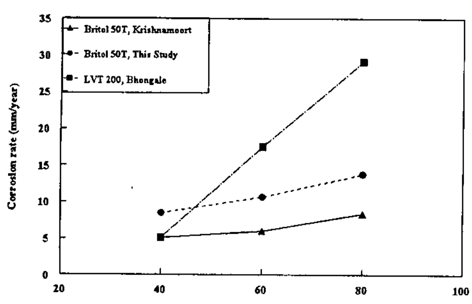

Figure 11: Effect of temperature on corrosion rate with different oils for 40 % water cut, Froude number 9 and total pressure of 0.79 MPa

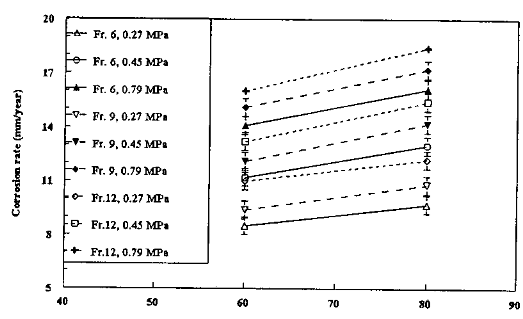

Figure 12: Variation of corrosion rate with temperature at 80 % water cut

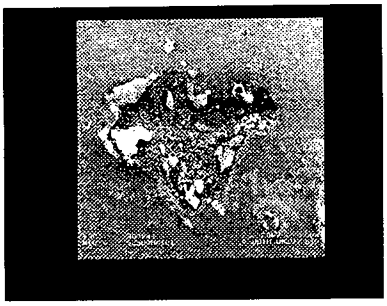

Figure 13: Corrosion film found on the surface of a coupon exposed to slug flow 0.27 MPa, 80 C, Froude number 12 and 80% water cut

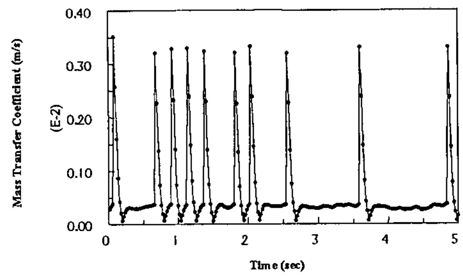

Fig14: Instantaneous Mass Transfer Coefficient vs Time at Froude number 9 in Slug Flow